Russian Geology and Geophysics © 2019, V.S. Sobolev IGM, Siberian Branch of the RAS
Vol. 60, No. 7, pp. 768–780, 2019 *DOI:10.15372/RGG2019045* *Geologiya i Geofizika*

A Borehole Record of Late Quaternary Permafrost on Kurungnakh Island (Lena Delta, Northeastern Siberia): Reconstruction of Deposition Environments

L.B. Khazin[a,b], I.V. Khazina[a], O.B. Kuzmina[a,b], D.E. Ayunov[a], N.A. Golikov[a,c], L.V. Tsibizov[a,b]

[a] *A.A. Trofimuk Institute of Petroleum Geology and Geophysics, Siberian Branch of the Russian Academy of Sciences, pr. Akademika Koptyuga 3, Novosibirsk, 630090, Russia*

[b] *Novosibirsk State University, ul. Pirogova 2, Novosibirsk, 630090, Russia*

[c] *Novosibirsk State Technological University, pr. Karla Marksa 20, Novosibirsk, 630073, Russia*

Received 26 December 2017; received in revised form 19 April 2018; accepted 25 April 2018

Abstract—Paleoenvironmenal reconstructions have been made from a multidisciplinary study of a borehole permafrost record on Kurungnakh Island (Lena delta). According to data on palynomorphs and ostracods, the clay silt units from the 10.58 to 13.54 m and 1.58 to 10.3 m core depth intervals were deposited in the Late Pleistocene (during the Karginian interstadial) and Early–Middle Holocene, respectively. The sediments were studied in terms of moisture contents, grain size distribution, mineralogy, and magnetic susceptibility, and the results were compared with published evidence from nearby natural outcrops. Quite a cold oligotrophic lake existed in the area during the Karginian period, and the deposition was interrupted by a gap recorded at a core depth of about 11 m. In the Early and Middle Holocene, the area was covered with shrub tundra vegetation.

Keywords: ostracod, palynomorph, moisture content, particle size distribution, magnetic susceptibility, Pleistocene, Holocene, Lena Delta, East Siberia

INTRODUCTION

The Lena Delta is among best documented parts of the Russian Arctic. It was a study area of multiple research projects, including those run jointly by Germany and Russia on the Laptev Sea System. The joint projects focused on geocryological and geological aspects of the delta and its surroundings (Schwamborn et al., 2002; Laptev Sea System, 2009; Bolshiyanov et al., 2013; etc.), as well as on paleoenvironmental reconstructions (Schwamborn et al., 2000; Andreev et al., 2002; Shirrmeister et al., 2003; Wetterich et al., 2005, 2008; etc.). The obtained multidisciplinary results, like pieces of a puzzle, provide an idea of the Late Pleistocene–Holocene history of the area. The present study is one such piece that extends the knowledge in several aspects: land and water vegetation on Kurungnakh Island coeval to deposition of the cored sediments; taxonomic diversity of ostracods in different periods; deposition environments.

Permafrost ecosystems are highly sensitive to global change (Vasil'chuk, 2007), and microfossil fauna from reference permafrost sections is a valuable climate proxy that has implications for depths and salinity of paleobasins and for vegetation in their surroundings. This information can be also used to predict the development of the Arctic region in the nearest future.

✉ Corresponding author.
E-mail adress: HazinLB@ipgg.sbras.ru (L.B. Khazin)

The reported study is based on core data from a 24.5 m deep borehole in a shallow thermokarst depression (alas) near Lake Udachnoe, southern Kurungnakh Island, Lena Delta (Fig. 1). The borehole was drilled in 2015 by a team from the A.A. Trofimuk Institute of Petroleum Geology and Geophysics (IPGG, Novosibirsk) to estimate the amount of permafrost degradation for the case of an alas. The core was documented at the Samoilovskii Research Station; water content and mass specific magnetic susceptibility were measured in the core immediately after recovery, and samples were selected for analyses of micropaleontology, grain size distribution, and mineralogy. The objectives included obtaining climate and environment paleoreconstructions, as well as age constraints by correlation of pollen spectra and ostracod assemblages with those from reliably dated natural outcrops in the vicinity of the drilling site (Wetterich et al., 2005, 2008; etc.).

PRESENT PHYSIOGRAPHIC CONDITIONS

The Lena Delta is located in the zone of Arctic continental climate, with a mean annual air temperature of –13 °C and monthly means of –32 °C for January and 6.5 °C for July, and a mean annual precipitation of 190 mm (Bolshiyanov et al., 2013). This is an area of 500–600 m thick continuous permafrost under a 30–50 cm seasonally thawing active layer.

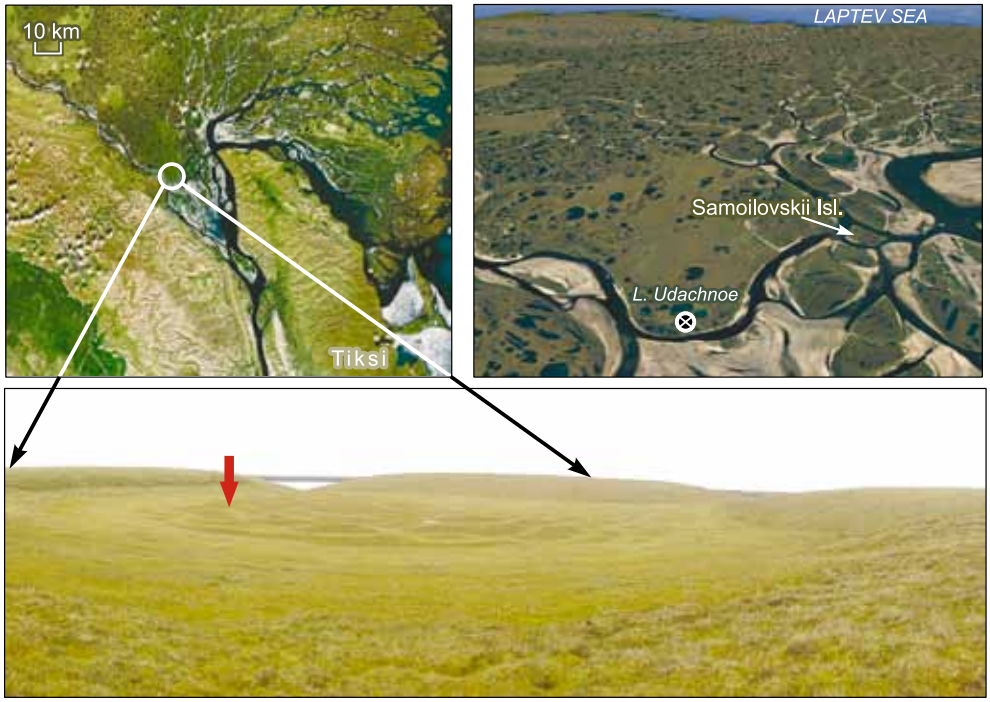

Fig. 1. Location map of borehole on Kurungnakh Island.

Almost the whole delta plain lies in tundra. Most of the territory is occupied by wet tundra landscapes dominated by sedges and mosses while other landscapes (dry sedge-moss and shrub tundra; wet moss-grass tundra; dry and wet shrub tundra; dry grass and hummocky tundra) are restricted to smaller areas; some local areas are bare (Schneider et al., 2009).

Extant ostracod assemblages of the East Siberian Arctic have been exhaustively studied (Wetterich et al., 2005, 2008, 2009; etc.), and ostracod communities typical of different water bodies, from rivers to thermokarst lakes were distinguished. Their taxonomy consists mainly of *Candona* and *Fabaeformiscandona* genera of the Candoninae subfamily, which are common Arctic inhabitants.

MATERIALS AND METHODS

Core section. The borehole was drilled and cored; the core diameter ranged from 136 mm in the upper 7 m to 117 mm between 7.0 and 22.3 m, and to 98 mm within 22.3–24.0 m. A 17 m long core was studied.

The section comprises several intervals (Fig. 2): peat on the top (0–0.6 m); mainly ice-rich clay silt with large and small ice veins and lenses or pore ice, locally with organic inclusions, between 0.6–9.5 m; dense frozen massive clay silt from 9.5 to 13.0 m; frozen massive medium-grained sand from 13.0 to 14.4 m; dense massive clay silt within 14.4–15.4 m; frozen massive sand at base (15.4–17.0 m).

Ostracods. Ostracod shells were isolated from 100 g specimens (standard size for Cenozoic samples) in order to provide commensurate counts. The sediment samples were wet sieved through a 0.067 mm mesh screen and then air dried. Valves were identified under a Zeiss Stemi 2000 binocular and photographed using a Zeiss Discovery V12 stereo zoom microscope. The collection is stored at the Laboratory of Micropaleontology of IPGG (Novosibirsk).

Palynology. Pollen spectra were studied in 57 samples selected from core depths between 0.92 and 16.8 m; satisfactory numbers of palynomorphs were found in 21 samples only. The samples were preconditioned following the method practiced at the Laboratory of Mesozoic and Cenozoic Paleontology and Stratigraphy (IPGG, Novosibirsk), using potassium pyrophosphate to remove clay particles and Cd heavy liquid (2.25 g/cm^3) to separate the organic and mineral components. Pollen and spores were identified in temporary and permanent preparation slides under a Zeiss Primo Star light microscope and photographed under a Zeiss Axioskop 40 light microscope using a Canon PowerShot G10 camera with ×400 and ×630 magnifications. The collection is stored at the Laboratory of Mesozoic and Cenozoic Paleontology and Stratigraphy (IPGG, Novosibirsk).

The percentages of pollen, as well as spores and nonpollen palynomorphs, are based on the sum of tree, shrub, and herb-shrub pollen. The contents of different components were estimated over at least 200 grains. The diagram was plotted using the *Tilia/TiliaGraph* software (Grimm, 1991). The palynomophs were identified using various guides (Bobrov et al., 1983; Komarek and Jankovska, 2001; Kupriyanova and Aleshina, 1972, 1978; Savel'eva et al., 2013; Ukraintseva, 1993; etc.).

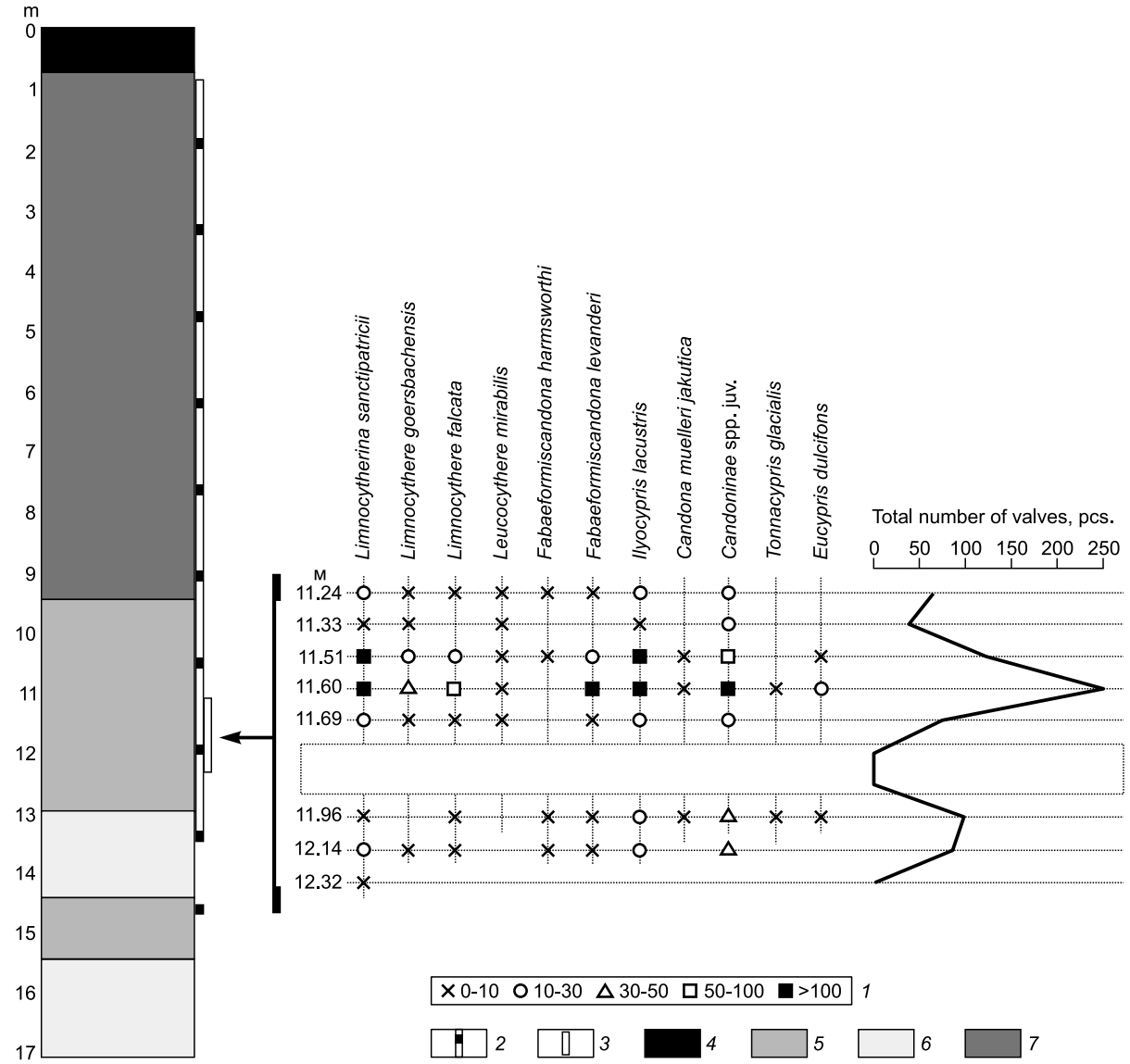

Fig. 2. Section structure and distribution of ostracods. *1*, number of pieces; *2*, pollen; *3*, ostracods; *4*, peat; *5*, compact loams; *6*, sandstones; *7*, loams.

Preliminary micropaleonotlogical results were published previously (Khazin et al., 2017).

Moisture content. Particle size distribution. Mineralogy. Ninety four core samples of permafrost were analyzed for total moisture content and percentages of sand-silt and clay size fractions; particle size distribution and mineralogy (XRD analysis) were determined in a few samples.

Moisture content was measured as percentages of vein and pore ice, pore and capillary water relative to the sample weight, following the State Standard GOST 5160- 2015.

Seven samples were analyzed in more detail for grain size distribution in the sand-silt fraction and for mineralogy in the clay fraction (<10 μm). The clay component was separated by decantation, and minerals were identified on a Thermo Scientific ARL X'TRA X-ray powder diffractometer.

Magnetic susceptibility. Volume specific magnetic susceptibility was measured in frozen samples immediately after core recovery, using a portable KT-5 kappameter, with a working frequency of 10 kHz and a sensitivity of 10^{-5} SI units (10^{-8} m^3/kg). The measurements (72 determinations in the 0.5 to 17 m depth interval) were applied to the core side surfaces; the data were corrected for surface curvature using a coefficient depending on the curvature radius according to the instrument specifications (Kappameter…, 1980).

RESULTS

Ostracods. Ostracods were found in clay silt (interval 11.24–12.98 m). Their taxonomy is quite diverse (Fig. 2, Plate 1): *Limnocytherina sanctipatricii* (Brady et Robertson), *Limnocythere goersbachensis* Diebel, *L. falcata* Diebel, *Leucocythere mirabilis* Kaufmann, *Fabaeformiscandona harmsworthi* (Scott), *F. levanderi* (Hirschmann), *Ilyocypris*

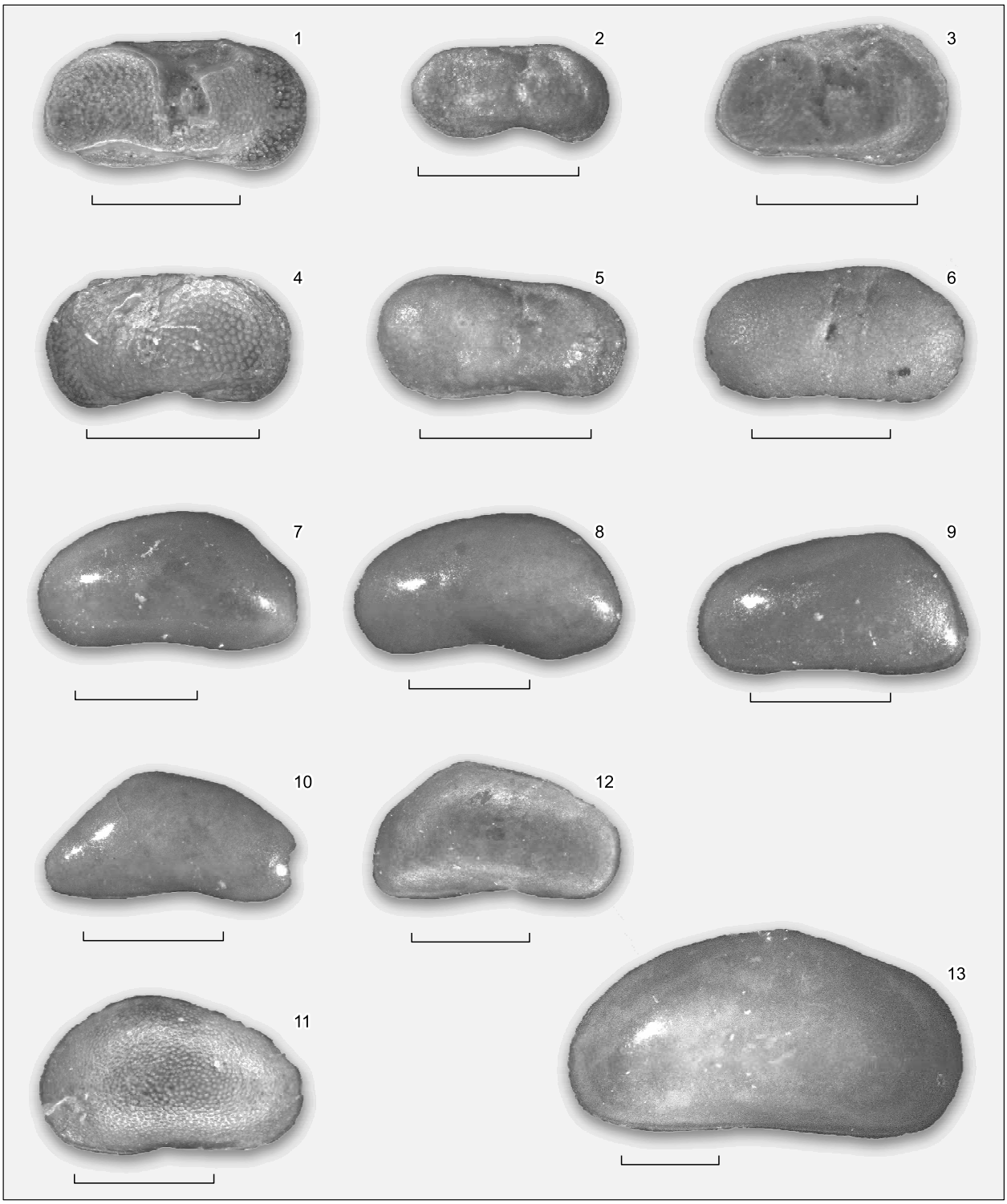

Plate 1. Ostracods from core samples. 1, *Limnocythere falcata* (right valve), 2, *Limnocythere goersbachensis* (male, right valve), 3, *Leucocythere mirabilis* (female, right valve); 4, 5, *Limnocytherina sanctipatricii* (4, female, left valve; 5, male, right valve); 6, *Ilyocypris lacustris* (right valve); 7, 8, *Fabaeformiscandona levanderi* (7, female, left valve; 8, male, left valve); 9, *Candona muelleri jakutica* (left valve); 10, *Candona* cf. *combibo* (right valve); 11, *Eucypris dulcifons* (female, left valve); 12, *Fabaeformiscandona harmsworthi* (female, right valve), 13, *Tonnacypris glacialis* (right valve). Scale bar is 0.5 mm.

lacustris Kaufmann, *I.* cf. *bradyi* Sars, *Candona muelleri jakutica* Pietrzeniuk, *Candona* cf. *combibo* Livental, *Candona* sp., Candoninae spp. juv., *Tonnacypris glacialis* (Sars), *Eucypris dulcifons* Diebel et Pietrzeniuk.

The assemblage consists of predominant *Limnocytherina sanctipatricii, Ilyocypris lacustris*; rather abundant *Limnocythere goersbachensis* and *Limnocythere falcate*; and only four species of the Candoninae subfamily, unlike the extant counterparts. All identified species are cold sthenothermic or oligo-thermophilic taxa, i.e., are unique to or preferring cold water environments (Meisch, 2000; Wetterich et al., 2005, 2009).

The sediments at 11.78–11.87 m lack ostracod shells but contain abundant plant remnants. This gap divides the ostracod record into the upper and lower subunits. In all other aspects, the conditions in the basin were stable, judging by high taxonomic diversity of ostracods.

Limnocytherina sanctipatricii was ubiquitous in lacustrine deposits from the Pleistocene in West Siberia, European Russia, Northern Europe, and the USA (Kazmina, 1975; Meisch, 2000). It is found in all samples with ostracod fauna but reaches especially high numbers (>100) in the upper part.

Leucocythere mirabilis is common in the upper subunit but is less abundant than the coexisting *Limnocytherina sanctipatricii* (Meisch, 2000). Both species live in cold oligotrophic lakes; *L. mirabilis* prefers deeper water (at least 12 m) though is present at shallower depths as well. In the Russian literature it is called *Limnocythere baltica* Diebel, which is junior synonym of *Leucocythere mirabilis* (Fuhrmann, 2012). *Limnocythere baltica* was reported from middle–upper Quaternary or occasionally from lower Quaternary sediments in West Siberia and in the northern Altai region (Kazmina, 1975).

Whole shells of *Tonnacypris glacialis* were found in two samples from the middle core depth interval (11.96–11.60 m). The southern boundary of its present habitat follows 65° N, while its presence in the assemblage indicates summer temperatures about 6 °C (Griffith et al., 1998).

Finally, *Ilyocypris lacustris*, another species found in abundance all over the core interval, prefers water temperatures about 4 °C (Fuhrmann, 2012).

Sample from the depth 11.6 m contains several valves looking like *Candona combibo* known from middle and upper Pleistocene deposits in West Siberia, northern Altai region, Kazakhstan, and Caucasus. *Candona combibo* remains were also found in the Black Sea Holocene bottom sediments (Buryndina and Bondar, 2012).

Thus, the ostracod taxonomy prompts the existence of a cold oligotrophic lake during the respective deposition period. It was originally quite shallow and rapidly became still shallower and vegetated, but its depth increased later on. The water temperatures were the coldest during the deposition of the middle part of the second unit with especially abundant *Ilyocypris lacustris* and juvenile Candoninae which failed to reach the reproductive stage because of unfavorable conditions.

Pollen spectra. Sand and clay silt in the 13.54–16.80 m interval lack spores and pollen, except for few conifer grains redeposited from pre-Quaternary sediments and small amounts of spore and pollen at 14.66 m. The latter pollen spectra contain tree and shrub species, mainly *Betula* sect. *Nanae*, *Betul*a sect. *Albae*, and *Alnus fruticosa*-type and few grains of conifers (*Picea* sp., *Pinus sylvestris* L., *Pinus* s/g *Haploxylon*), herb-shrub species (Ericaceae, Caryophyllaceae, Poaceae), as well as spores of *Sphagnum* sp., *Bryales*, Polypodiaceae.

Pollen assemblage 1 from clay silt at 10.58–13.54 m has high percentages of herb-shrub pollen and microphytoplankton (Fig. 3, Plate 2).

The spectra most often contain predominant *Artemisia* sp., Cyperaceae, and Poaceae; moderate amounts of Caryophyllaceae, Asteraceae, *Thalictrum* sp., *Polygonum bistorta*-type, Saxifragaceae, Ranunculaceae, *Valeriana* sp., *Polemonium* sp., Apiaceae, Papaveraceae, *Rubus chamaemorus* L., etc.; small percentages of trees and shrubs, mainly *Betula* sect. *Nanae*, *Betula* sect. *Albae, Betula* spp., *Alnus fruticosa*-type, *Salix* sp., *Pinus* spp., and *Picea* sp, as well as minor amounts of spores: *Lycopodium annotinum*-type, *L. clavatum*-type, *Bryales, Selaginella rupestris* (L.) Spring, Polypodiaceae, *Sphagnum* sp., *Encalypta* sp.

Microphytoplankton is abundant and belongs to green algae: *Pediastrum boryanum* (Turpin) Meneghini, *Pediastrum* spp., *Botryococcus* sp., *Spirogyra* sp., and Zygnemataceae.

Assemblage 1 records vegetation of forest-free open spaces occupied with steppe and tundra communities. High percentages of algae (*Pediastrum* and *Botryococcus*) record the existence of a clear fresh lake.

The spectra of clay silt in the 10.30–10.58 m interval show minor percentages of *Alnus fruticosa*-type, *Betula* spp., *Betula* sect. *Nanae*, *Pinus* spp., Ericaceae, Poaceae, Cyperaceae, etc.

Pollen assemblage 2 from clay silt in the 1.58–10.30 m core interval comprises predominant tree and shrub pollen and spores (Fig. 3, Plate 3).

The tree-shrub species are most often *Betula* spp. and *Betula* sect. *Nanae*, minor amounts of *Alnus* sp., *Alnus fruticosa*-type, and few grains of *Salix* sp.

The spores are predominant *Sphagnum* sp. and minor Polypodiaceae, *Lycopodium annotinum*-type, *L. clavatum*-type, *Selaginella rupestris*, *Encalypta* sp.

Herb-shrub vegetation consists mainly of Ericaceae, with minor amounts of Apiaceae, Asteraceae, *Artemisia* sp., Caryophyllaceae, Cyperaceae, *Thalictrum* sp., Poaceae, Onagraceae, and Saxifragaceae.

Nonpollen palynomorphs include *Pediastrum boryanum* (especially abundant at 2.9 m), *Pediastrum* spp., Zygnemataceae, *Spirogyra* sp., *Botryococcus* sp., Fungi, *Glomus* sp.; diatoms were found in a sample from 1.58 m.

Judging by these spectra, the territory was covered by shrub tundra vegetation during the deposition of the 1.58–10.30 m interval.

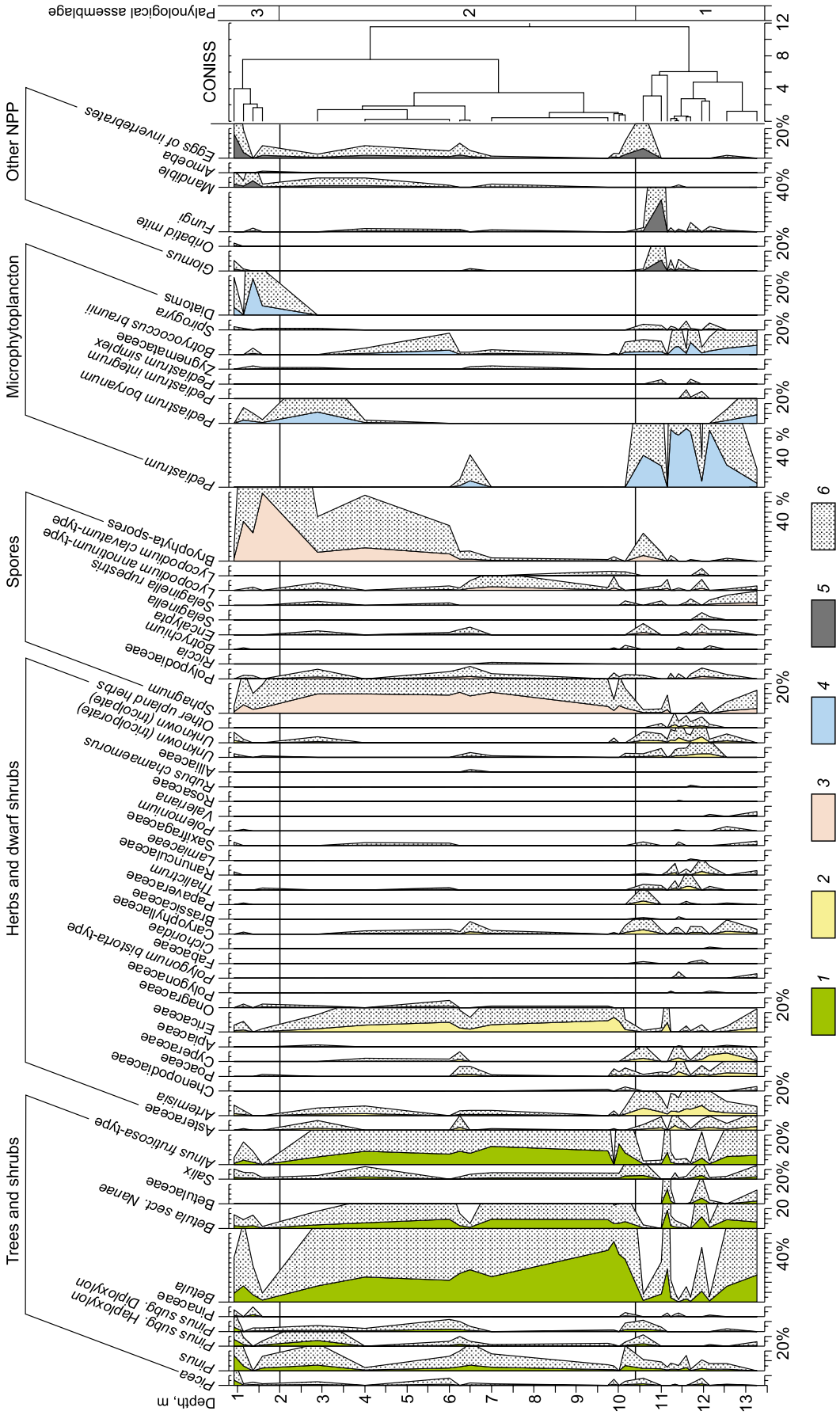

Fig. 3. Pollen diagram. *1*, trees and high shrubs; *2*, herbs and low shrubs; *3*, spores; *4*, microphytoplankton; *5*, nonpollen polymorphs; *6*, contents with index 5.

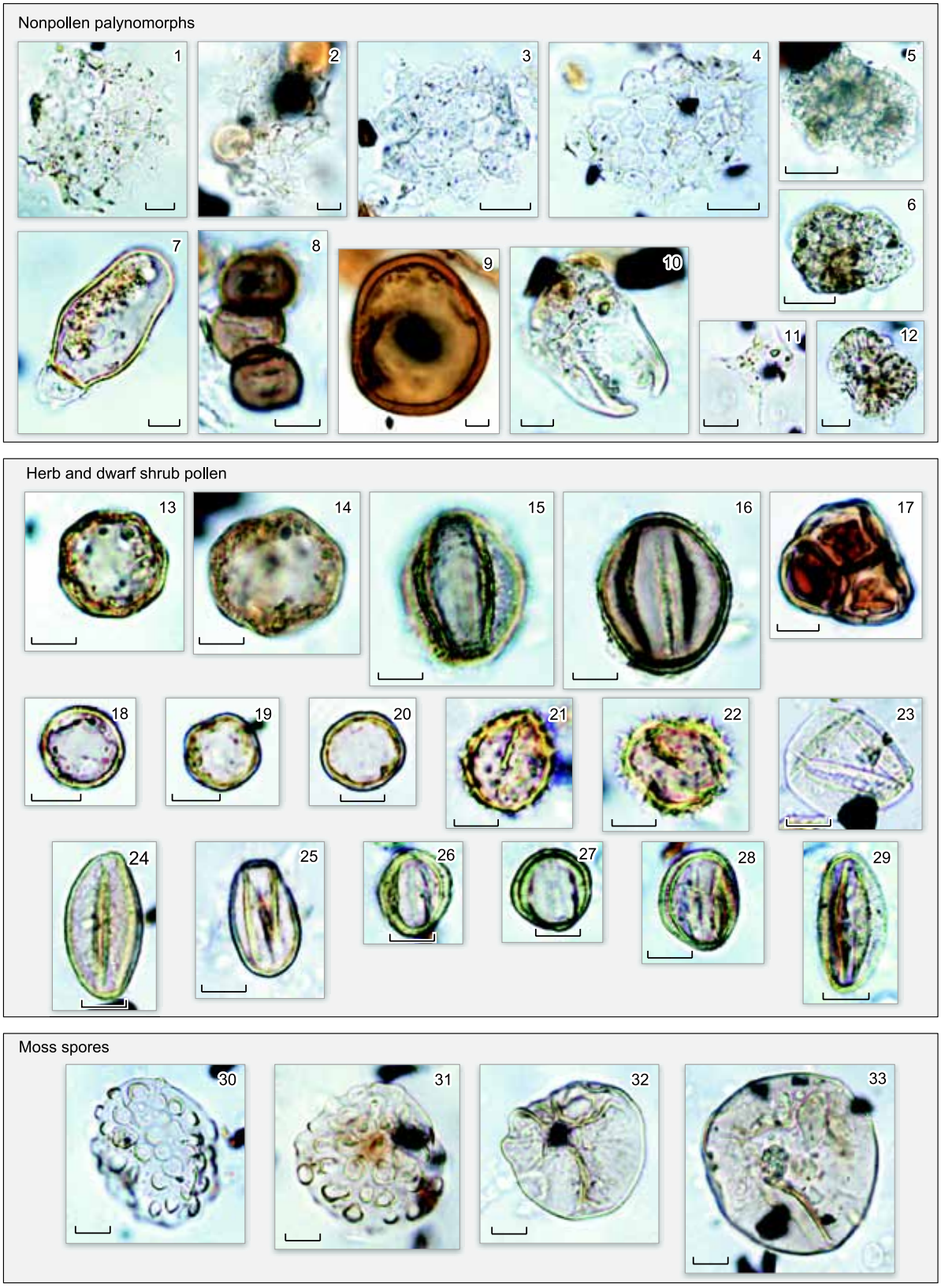

Plate 2. Palynomorphs predominant in pollen assemblage 1. Scale bar is 10 μm. 1, *Pediastrum boryanum*; 2, *Pediastrum* cf. *integrum*; 3, 4, *Pediastrum* sp.; 5, 6, *Botryococcus* sp.; 7, Rhizopoda; 8, Fungal spore; 9, *Glomus* sp.; 10, Mandible; 11, Acritarha (?); 12, *Botryococcus* cf. *neglecta*; 13, 14, Caryophyllaceae; 15, 16, *Rubus chamaemorus*; 17, Ericaceae; 18–20, *Thalictrum* sp., 21, 22, Asteraceae; 23, Cyperaceae; 24, Ranunculaceae; 25, Tricolpate pollen; 26–28, *Artemisia* sp.; 29, Tricolporate pollen; 30, 31, *Encalypta* sp.*;* 32, 33, *Selaginella rupestris.*

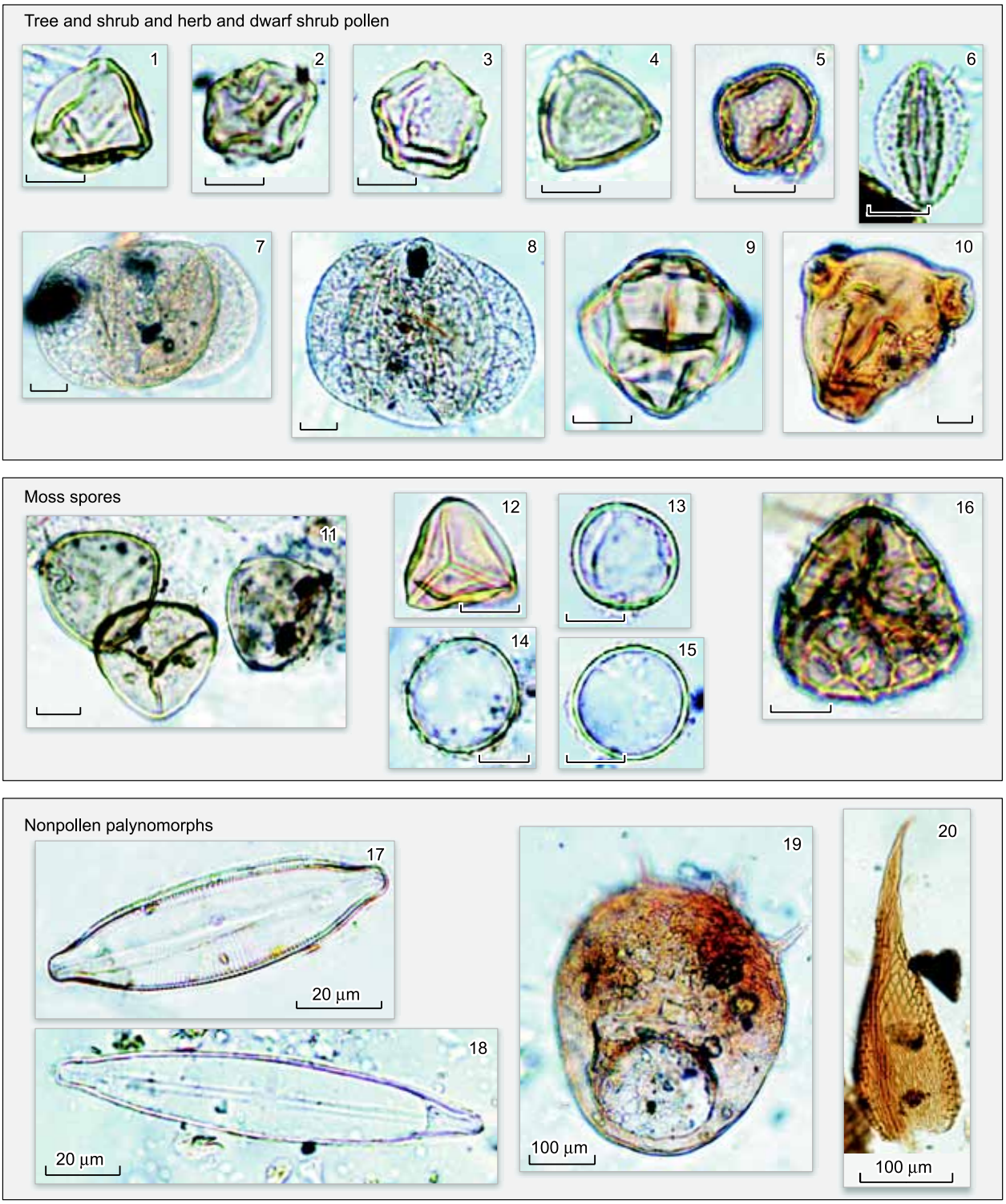

Plate 3. Palynomorphs predominant in pollen assemblages 2 and 3. Scale bar is 10 µm; for some taxa, scale is shown in images. 1, 4, *Betula* sp.; 2, 3, *Alnus fruticosa*-type; 5, 6, *Salix* sp.; 7, 8, *Pinus* s/g *Haploxylon*; 9, Ericaceae; 10, Onagraceae; 11, 12, *Sphagnum* sp.; 13–15, Bryophyta; 16, *Lycopodium annotinum*-type; 17, 18, Diatoms; 19, Rhizopoda; 20, *Sphagnum*.

Pollen assemblage 3 from clay silt in the core top (0.92–1.58 m) contains more green moss spores and less Ericaceae than below, as well as sphagnum spores and larger amounts of nonpollen palynomorphs. The spectra show minor percentages of *Betula* sect. *Nanae*, *Betula* sect. *Albae*, *Alnus fruticosa*-type, but higher percentages of conifers. Herbs and shrubs are likewise minor; Ericaceae grains are much fewer than in assemblage 2; Caryophyllaceae, Poaceae, Pa-

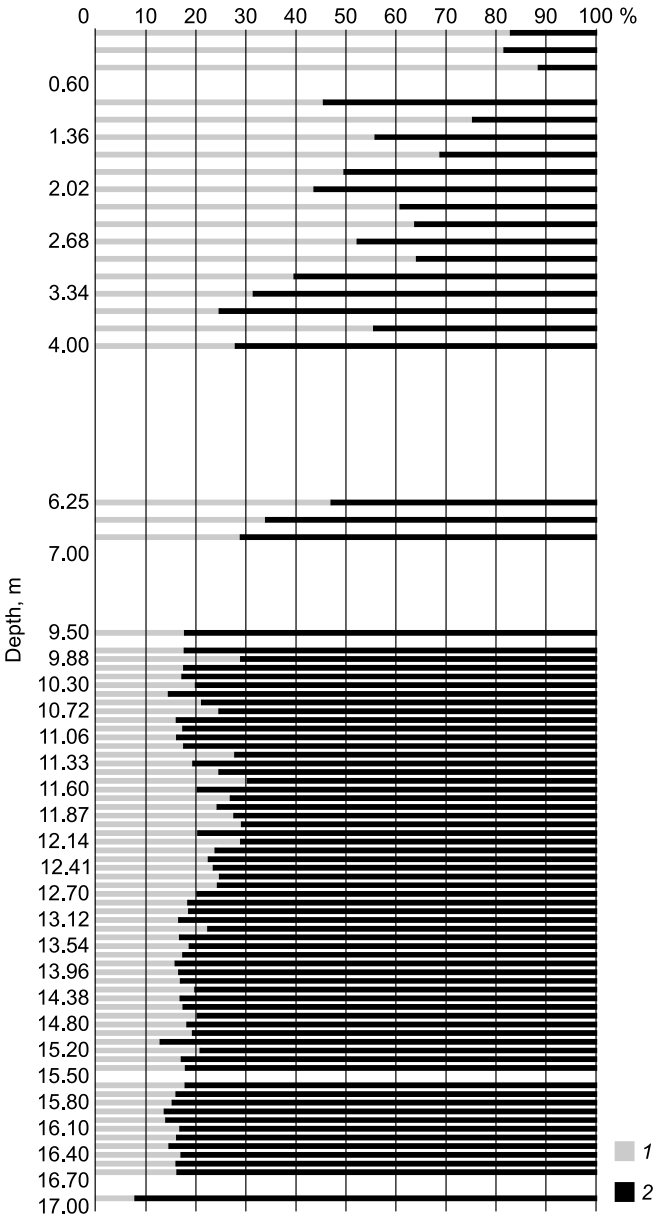

Fig. 4. Relative percentages of moisture (*1*) and mineral component (*2*) in the section.

paveraceae, Asteraceae, *Artemisia* sp., Onagraceae, Saxifragaceae, *Thalictrum* sp. etc. occur as few grains.

Microphytoplankton taxa include *Pediastrum boryanum, Pediastrum* sp., Zygnemataceae, *Spirogyra* sp., and *Botryococcus* sp. Diatoms are abundant in some samples (Plate 3). Nonpollen palynomorphs, such as Fungi, *Glomus* sp., and Pseudoshizaea are more abundant than in assemblage 2. The samples also bear mouth parts (mandible) and eggs of invertebrates, and soil mite. Spores comprise predominant Bryophyta, lesser amounts of *Sphagnum* sp., and minor Lycopodiaceae, Polypodiaceae, and *Encalypta* sp.

The assemblage taxonomy indicates a wet open tundra landscape.

Moisture content. The moisture contents behave in different ways in 17–7 m and 7–0 m intervals: they are stable and average about 20% (Fig. 4), mainly at the account of pore ice, in samples from the lower unit but are variable in the upper unit, increasing gradually upward. Sediments in the upper four meters enclose lenses and veins of transparent ice which produce layered and reticulate cryostructures. Locally there are dipping parallel up to 7 mm thick veins of transparent ice that crosscut the sediments. The moisture content reaches 80% in the uppermost one meter at the account of vein and pore ice.

Lithology. In terms of sand-silt and clay contents, the section likewise comprises two units (Fig. 5, left): sands from 17 to 13 m and clay silt above (13.0–0.9 m). The lower unit consists of almost pure sand (>98%), with few clay silt interbeds at 13 and 15 m. The upper clay silt unit is composed of clay (~50%) and clay-silt (~50%) fractions, but the latter predominates at 3.3–4.0 m (about 80%) and 10.4 m (84%).

Particle sizes. The sediments fall into three groups according to particle size distribution (Fig. 5, right): lognormal distribution from 0.26 to 1.80 m, 100–120 μm (samples 4–18, 4–10); a more complex distribution corresponding to dense clay silt at 6.25, 10.02 and 12.5 m (samples 7–4, 11–8, 12–2, respectively); lognormal distribution at the section base, where ~230 μm pure sand was recovered from 14.1 and 15.2 m core depths (samples 4–18 and 4–10, respectively).

Particle sizes, along with clay contents, record different deposition environments. The lower unit of homogeneous sand was deposited in flowing conditions; heterogeneous sediments in the middle result from turbiditic deposition, and the section top with high clay contents formed in stable water.

Mineralogy. The XRD analysis shows quite uniform mineralogy (Table 1). Quartz predominates in the sand-silt fraction and reaches about 50% (above 12 m) or more (below 12 m) in clay particles. The percentage of plagioclase is 20–25% on average. The clay fraction contains also K feldspar and muscovite (5–7% each) and 7–10% chlorite between 0.26 and 6.25 m, but the respecive contents are lower in the lower unit (5, 5 and 5–7%). Minor phases include amphibole (all along the section), siderite, and illite-smectite (locally). In general, the high percentage of quartz in all fractions indicates that the clay component is derived from sand-silt material. The poor diversity of minerals and low polymicticity may be evidence of repeated erosion and redeposition of transported sediments.

Magnetic susceptibility. The volume specific magnetic susceptibility (κ) of sediments generally increases with depth (Fig. 6). It is relatively low (~10^{-4} SI units) in the upper unit from 0.5 to 8.0 m, because percentages of ferromagnetic minerals (magnetite and hematite) in the heavy fraction are low. Furthermore, the shallow sediments are wet and ice-rich (~50% moisture, Fig. 6), while ice is weakly diamagnetic with a susceptibility of ~ -10^{-5} SI units (Lonsdale, 1949). Magnetic susceptibility increases from 0.5 ×

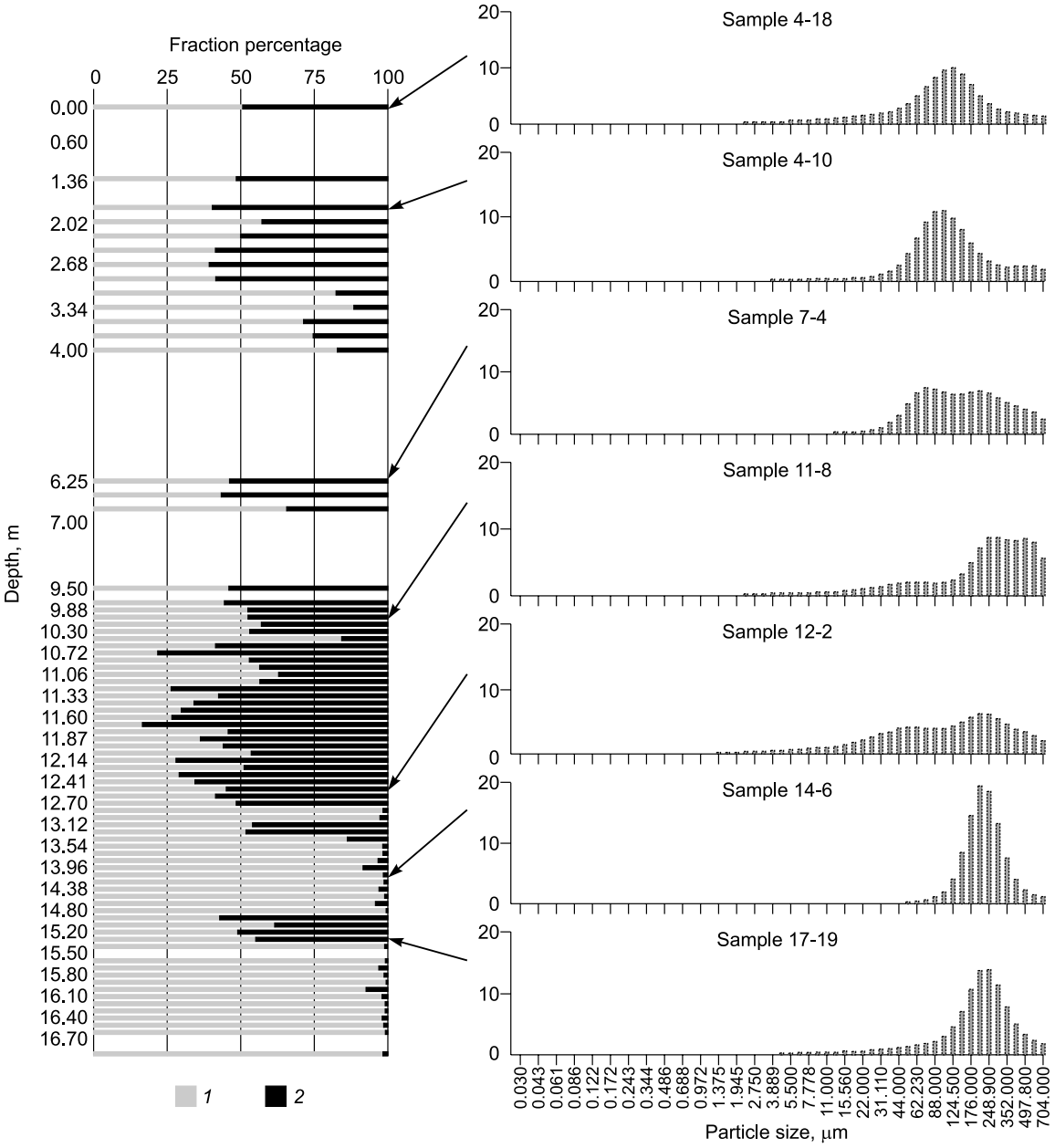

Fig. 5. Sand-silt (*1*) and clay (*2*) fractions (left) and particle sizes (%) of sand-silt fraction (right).

10^{-3} to 1.5×10^{-3} SI units between 11 and 17 m, where the moisture content remains within 20%. Therefore, the contribution of the ferromagnetic component increases depthward. The behavior of magnetic susceptibility differs from the general pattern within the 9.7–10.4 m interval: it decreases from 0.6×10^{-3} to 0.3×10^{-3} SI units with depth but does not show any evident correlation with moisture variations.

DISCUSSION

Stratigraphy and paleoenvironment reconstructions.

Lower unit. Pollen assemblage 1 correlates well with assemblages of pollen zones PZ 1 and PZ 2 revealed in the natural outcrop on Kurungnakh Island (Wetterich et al., 2008), with their pollen spectra containing abundant herbs (Poaceae, Cyperaceae, *Artemisia*, Caryophyllaceae and lower percentages of Asteraceae, Thalictrum and Cruciferae) and microphytoplankton species *Pediastrum* and *Botryococcus*. The sediments that contain the PZ 1 and PZ 2 assemblages have AMS ^{14}C ages between 45,500 and 32,000 years BP and belong to the Karginian stage of the regional stratigraphy (Volkova and Borisova, 2010). At the time of deposition, plant communities of open steppe and tundra grew in the territory, while the presence of green algae records stable aquatic conditions (Wetterich et al., 2008). A similar environment was reconstructed for the Karginian interstadial

Table 1. Mineralogy according to XRD analysis of clay fraction (<0.001 mm)

Sample (core depth, m)	Quartz	Plagioclase	Chlorite	Dioctahedral mica (muscovite type)	K feldspar	Amphibole	Siderite	Illite-smectite
	%							
4–18 (0.26)	~50	20–25	7–10	5–7	5–7	Traces	–	–
4–10 (1.8)	~50	20–25	7–10	5–7	5–7	Traces	Traces	Minor amount
7–4 (6.25)	~50	20–25	10	5–7	5–7	Traces	Minor amount	Minor amount
11–8 (10.02)	~50	30–35	5–7	5	5	Minor amount	–	Traces
12–2 (12.5)	50–60	20–25	5–7	5	5	Traces	–	–
14–6 (14.1)	50–65	15–20	5	5	5	Minor amount	Traces	–
17–19 (15.2)	50–60	~25	5–7	5	5	3–5	–	–

in the Bykovsky Peninsula (Andreev et al., 2002). Thus, pollen assemblage 1 presumably represents Karginian time.

The ostracod assemblage is similar to assemblage 2 from a natural outcrop at the Mamontovy Khayata locality in taxonomy and taxa percentages (Wetterich at al., 2005). The age of the respective 8.8–22.0 m depth interval is bracketed between 48,000 and 34,000 years BP. Correspondingly, the Kurungnakh cored sediments from the interval 11.24–12.98 m were deposited in the latest Late Pleistocene, during the Karginian interstadial.

These inferences based on ostracod and pollen evidence are supported by magnetic susceptibility data. The general pattern of depth-dependent κ variations is consistent with the results reported by Wetterich et al. (2008): stable low κ values in the upper unit (0–20 m according to Wetterich et al. (2008) and 0.5–7.0 m in this study) and gradual κ increase below (20–30 m in (Wetterich et al., 2008) and 11–17 m in this study). Wetterich et al. (2008) explain the depthward magnetic susceptibility increase in the ice complex by changes in the sediment source and in the transport distance. Denser particles with ferromagnetic minerals are transported to shorter distances than light-weight particles, and the concentration of ferromagnetics decreases as particles travel longer distances during erosion. It is difficult to quantitatively correlate our data with the results of Wetterich et al. (2008), because they studied dry material while we analyzed permafrost samples. Furthermore, we discuss the ice complex deposits that were strongly altered upon thawing. Note additionally that monotonic κ decrease from 0.6×10^{-3} to 0.3×10^{-3} SI units in the 9.7–10.6 m interval may result from aeration-related formation of strongly magnetic minerals (Babanin and Khudyakov, 1972; Kosnyreva, 2007) and record a long deposition gap with soil formation.

All above data indicate that a cold oligotrophic lake surrounded by forestless open spaces of tundra and steppe existed in the area in Karginian time.

The layer free from ostracods but containing abundant plant remnants may be evidence of lake shoaling and vegetation. This inference agrees with pollen data: higher percentages of nonpollen palynomorphs like conidiospores of *Glomus* and other Fungi spores (including *Multicellate*-type), as well as remnants of eggs and mouth parts of invertebrates. Such taxa are commonly found in surface soil samples and are evidence of erosion. A deposition gap is likewise inferred from κ behavior typical of soil formation processes.

Upper unit. Pollen assemblage 2 found in clay silt within the 1.58–10.3 m core depth interval correlates with the assemblage of zone PZ 4 from exposed Quaternary deposits on Kurungnakh Island (Wetterich et al., 2008). Greater percentages of *Alnus fruticosa*-type, *Betula* sect. *Nanae*, *B.* sect. *Albae* and Ericales in the pollen spectra of PZ 4 were attributed (Wetterich et al., 2008) to Early Holocene climate

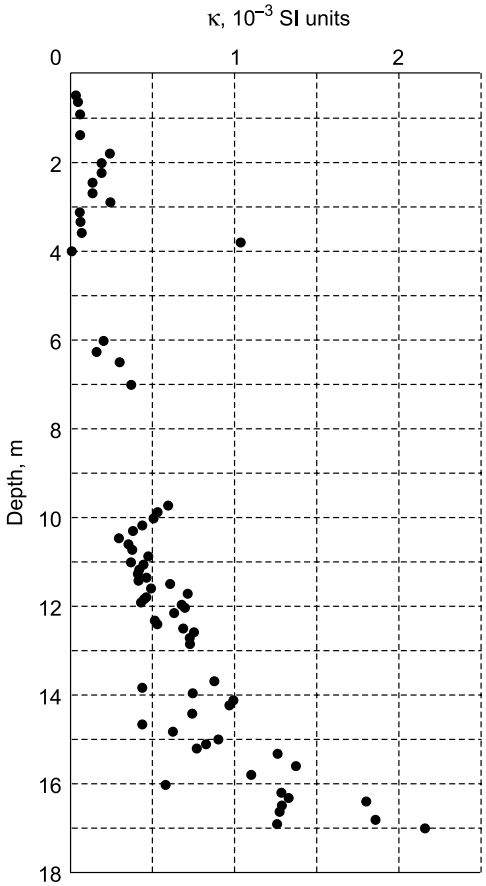

Fig. 6. Variations of magnetic susceptibility (κ).

amelioration. The same inference was suggested for pollen spectra from the Bykovsky Peninsula (Andreev et al., 2002). More favorable Early Holocene climate conditions are consistent with the presence of birch and larch trunks and their ages in the Lena Delta head, in the Bykovsky Peninsula, and on the Van'kina Bay coast (Bolshiyanov et al., 2013). Therefore, the forest line 8.9–8.6 kyr BP shifted toward the delta and into the adjacent areas; the forest of that time consisted of both larch and birch and formed during the Holocene climate optimum at 8900–8000 years BP.

The sediments with pollen of PZ 4 have AMS ^{14}C ages of 8.0 and 5.9 kyr BP (Wetterich et al., 2008). Thus, pollen assemblage 2 in the core section may belong to the early-middle Holocene.

The magnetic susceptibility and water content values in this unit vary in large ranges, which may evidence of unstable deposition conditions.

Pollen data show diverse plant communities (green moss, diatoms, Fungi spores, etc.) different from those in the sediments below, likely as a result of periodic water level changes.

CONCLUSIONS

According to the reported multidisciplinary data, the lower section part (17–10 m) was deposited during the Karginian interstadial in the latest Late Pleistocene, while the upper unit formed in the middle Holocene. At that time, a cold oligotrophic lake existed within the territory and was surrounded by open tundra and steppe landscapes. Vegetation in the early and middle Holocene mostly consisted of tundra shrub communities.

The deposition was interrupted by a gap, which is supported by paleontological and geophysical data.

The work was carried out as part of the basic program Interdisciplinary Integrate Research, project Comprehensive Characterization of Permafrost from Remote Sensing, Geological, Geophysicsl, Geobotanical, and Soil Studies, Research Station Samoilovskii run by the Siberian Branch of the Russian Academy of Sciences.

REFERENCES

Andreev, A., Schirrmeister L., Siegert, K., Bobrov, A., Demske, D., Seiffert, M., Hubberten, H.W., 2002. Paleoenvironmental changes in Northeastern Siberia during the Late Quaternary—evidence from pollen records of the Bykovsky Peninsula. Polarforschung 70, 13–25.

Babanin, V.F., Khudyakov, O.I., 1972. Magnetic susceptibility of permafrost-taiga soils in the Magadan region. Vestnik MGU, Ser. Biologiya, Pochvovedenie, No. 5, 88.

Bobrov, A.E., Kupriyanova, L.A., Litvintseva, M.V., Tarasevich, V.F., 1983. Spores of Pteridosperms and Pollen of Gymnosperms and Monocotiledons in the Flora of the European USSR [in Russian]. Nauka, Leningrad.

Bolshiyanov, D.Yu., Makarov, A.S., Schneider, V., Stof, G., 2013. Origin and Evolution of the Lena Delta [in Russian]. AANII, St. Petersburg.

Buryndina, L.V., Bondar, E.A., 2012. Holocene ostracod assemblages from the Black and Azov Seas (Russian sector), in: Modern Micropaleontology, Proc. XV All-Russian Conf., Gelendzhik, September 2012, pp. 223–226.

Fuhrmann, R., 2012. Atlas quartärer und rezenter Ostrakoden Mitteldeutschlands. Altenburger Naturwissenschaftliche Forschungen 15.

Griffith, H.I., Pietrzeniuk, E., Fuhrmann, R., Lennon, J.J., Martens, K., Evans, J.G., 1998. Tonnacypris glacialis (Ostracoda, Cyprididae): taxonomic position, (palaeo-) ecology, and zoogeography. J. Biogeography 25, 515–526.

Grimm, E., 1991. Tilia and Tiliagraph. Illinois State Museum, Springfield, IL, USA,

Kappameter model KT-5, 1980. User's Manual. Geofyzika Brno, Czechoslovakia.

Kazmina, T.A., 1975. Pliocene and Early Pleistocene Stratigraphy of the Southern West Siberia (Trans. IGiG SO AN SSSR, Issue 264) [in Russian]. Nauka, Novosibirsk.

Khazin, L.B., Khazina, I.V., Kuzmina, O.B., 2017. A borehole permafrost record of micropaleontology (ostracods, palynomorphs) on Kurungnakh Island (Lena Delta, Northeastern Siberia), in: Subsoil Use. Mining. Lines and Technologies of Mineral Exploration. Economy and Geoenvironment, Interexpo GEO-Sibir-2017, XIII Int. Conf. (Novosibirsk, 17–21 April 2017), A Collection of Papers, Vol. 1, pp. 7–11.

Komarek, J., Jankovska, V., 2001. Review of the Green Algal Genus Pediastrum; Implication for Pollen-Analytical Research. Berlin; Stuttgart, Cramer.

Kosnyreva, M.V., 2007. Integration of Geophysical Methods for Soil Mapping Applications. PhD Thesis [in Russian]. Moscow.

Kupriyanova, L.A., Aleshina, L.A., 1972. Pollen and Spores of the European USSR Flora [in Russian]. Nauka, Leningrad.

Kupriyanova, L.A., Aleshina, L.A., 1978. Pollen of Dycotiledon Plants, Lamiaceae—Zygophyllaceae, in the European USSR [in Russian]. Nauka, Leningrad.

Laptev Sea System, 2009. The System of the Laptev Sea and Adjacent Arctic Seas: Modern Environment and Paleoclimate [in Russian]. Mosk. Gos. Univ., Moscow.

Lonsdale, K., 1949. Diamagnetic susceptibility and anisotropy of ice. Nature 164, 101.

Meisch, C., 2000. Freshwater Ostracoda of Western and Central Europe. Subwasserfauna von Mitteleupora 8/3. Spektrum Akademischer Verlag, Heidelberg.

Savel'eva, L.A., Rashke, E.A., Titova, D.V., 2013. Photographs of Plants and Pollen from the Lena Delta. An Atlas [in Russian]. St. Petersburg.

Schirrmeister, L., Grosse, G., Schwamborn, G., Andreev, A., Meyer, H., Kunitsky, V., Kuznetsova, T., Dorozhkina, M., Pavlova, Y., Bobrov, A., Oezen, D., 2003. Late Quaternary history of the accumulation plain North of the Chekanovsky Ridge (Lena Delta, Russia): a multidisciplinary approach. Polar Geography 27 (4), 277–319.

Schneider, J., Grosse, G., Wagner, D., 2009. Land cover classification or tundra environments in the Arctic Lena Delta based on Landsat ETM + data and its application for upscaling of methane emissions. Remote Sensing Environment 113, 380–391.

Schwamborn, G., Andreev, A., Rachold, V., Hubberten, H.W., Grigoriev, M.N., Tumskoy, V., Pavlova, E.Yu., Dorozkhina, M.V., 2000. Evolution of Lake Nikolay, Arga Island, Western Lena River Delta, during Late Pleistocene and Holocene time. Polarforschung 70, 69–82.

Schwamborn, G., Rachold, V., Grigoriev, M., 2002. Late Quaternary sedimentation history of the Lena Delta. Quat. Int. 89, 119–134.

Ukraintseva, V.V., 1993. Vegetation Cover and Environment of the "Mammoth Epoch" in Siberia. Inc. Hot Springs, South Dakota.

Vasilchuk, A.C., 2007. Palynology and Chronology of Ice Wedge Complexes in Permafrost [in Russian]. Moscow University Press, Moscow.

Volkova, V.S., Borisova, B.A. (Eds.), 2010. Unified Quaternary Stratigraphy of Central Siberia (Taimyr, Siberian Platform). Explanatory Note [in Russian]. SNIIGGiMS, Novosibirsk.

Wetterich, S., Schirrmeister, L., Pietrzeniuk, E., 2005. Freshwater ostracods in Quaternary permafrost deposits in the Siberian Arctic. J. Paleolimnol. 34, 363–376.

Wetterich, S., Kuzmina, S., Andreev, A.A., Kienast, F., Meyer, H., Schirrmeister, L., Kuznetsova, T., Sierralta, M., 2008. Palaeoenvironmental dynamics inferred from late Quaternary permafrost deposits on Kurungnakh Island, Lena Delta, Northeast Siberia, Russia. Quat. Sci. Rev. 27, 1523–1540.

Wetterich, S., Schirrmeister, L., Andreev, A., Pudenz, M., Plessen, B., Meyer, H., Kunitsky,V.V., 2009. Eemian and Late Glacial/Holocene palaeoenvironmental records from permafrost sequences at the Dmitry Laptev Strait (NE Siberia, Russia). Palaeogeogr. Palaeoclimatol. Palaeoecol. 279, 73–95.

Editorial responsibility: N.V. Sennikov